Electronic Supplementary Information (ESI):

Photophysical properties and dynamics of donor–acceptor–heavy-atom molecules and their application in triplet–triplet annihilation upconversion

Jun Ho Yoon,[†a] Jeong-Min Park,[†b] Jae Moon Lee,[a] Hong Mo Kim,[a] Woo Jin Choi,[a] Hyun Kyu Lee,[a] Suhyeon Kim,[a] Wan Soo Kim,[a] Min Sung Kim,[a] Yoo Sang Kim,[a] Dong Jun Lee,[a] Yoona Noh,[c] Juwon Oh,*[c] Jae-Hyuk Kim*[b] and Jae Pil Kim*[a]

[a] *Department of Materials Science and Engineering, Seoul National University, Seoul, 08826, Republic of Korea*

[b] *Department of Civil and Environmental Engineering, Pusan National University, Pusan, 46241, Republic of Korea*

[c] *Department of Chemistry, Soonchunhyang University, Asan, 31538, Republic of Korea*

[†] *These authors contributed equally to this work.*

[*] *Corresponding author.*

E-mail: jaepil@snu.ac.kr

Table of contents

1. Synthesis procedures

Synthesis of PY-BDP

A solution of 1-pyrenecarboxaldehyde (2.30 g, 9.988 mmol, 1 eq) and 2,4-dimethylpyrrole (3.08 mL, 29.966 mmol, 3 eq) in dry CH_2Cl_2 (550 mL) was mixed with a solution of trifluoroacetic acid (153.05 μL, 2 mmol) in dry CH_2Cl_2 (10 mL) at room temperature under N_2 atmosphere. After 1.5 h, p-chloranil (2.22 g, 9 mmol) was added while cooling on ice and stirred for 10 min. After another hour, triethylamine (8 mL) was added followed by $BF_3 \cdot Et_2O$ (8 mL), and the mixture was stirred for an additional 2 h before being poured into water. After extraction, the organic layer was dried over anhydrous $MgSO_4$, and then evaporated under reduced pressure to obtain the crude product. To purify the crude product, column chromatography was performed using silica gel and a mixture of CH_2Cl_2/*n*-hexane (2:1, v/v) as the eluent. This process resulted in the production of orange solid PY-BDP, with a yield of 12% (537 mg). ^{1}H NMR (500 MHz, Chloroform-d): δ (ppm) 8.50–8.48 (d, J=7.85 Hz, 1H), 8.41–8.39 (d, J=7.55 Hz, 1H), 8.35–8.33 (d, J=7.25 Hz, 1H), 8.31 (s, 2H), 8.24–8.22 (d, J=9.20 Hz, 1H), 8.16–8.12 (t, J=7.65 Hz, 1H), 8.05–8.04 (d, J=7.85 Hz, 1H), 7.86–7.84 (d, J=9.15 Hz, 1H), 6.16 (s, 2H), 2.50 (s, 6H), 0.83 (s, 6H). ^{13}C NMR (850 MHz, Chloroform-d): δ (ppm) 155.29, 142.53, 140.33, 131.47, 131.38, 130.75, 130.36, 129.27, 128.43, 128.33, 127.30, 126.84, 126.10, 125.98, 125.90, 125.71, 123.81, 123.62, 123.13, 121.53, 40.00, 39.83, 39.66, 39.49, 39.33, 39.16, 38.99, 14.31, 13.31. GC/HRMS (EI) calculated for $C_{29}H_{23}BF_2N_2$: 448.1922, found: 448.1923.

Synthesis of PY-BDP-2Cl

N-Chlorosuccinimide (NCS) (27 mg, 0.200 mmol, 5 eq) in CH_2Cl_2 (6 mL) was slowly added dropwise to PY-BDP (18 mg, 0.040 mmol) in 10 mL of dry CH_2Cl_2 within 0.5 h. The resulting mixture was stirred for an additional 12 h, washed with a sodium chloride aqueous solution, and extracted with CH_2Cl_2. The organic layers were combined, dried with $MgSO_4$, and then evaporated until dryness. The orange solid product PY-BDP-2Cl was obtained with a 40% yield (8.25 mg) through column chromatography

on silica gel, using CH_2Cl_2/*n*-hexane (3:2, v/v) as the eluent. ^{1}H NMR (500 MHz, Chloroform-d): δ (ppm) 8.32–8.30 (d, J=6.50 Hz, 1H), 8.29–8.28 (d, J=6.30 Hz, 1H), 8.24–8.23 (d, J=6.10 Hz, 1H), 8.21–8.20 (d, J=7.45 Hz, 1H), 8.16–8.15 (d, J=7.45 Hz, 1H), 8.09–8.06 (m, 2H), 7.95–7.93 (d, J=7.60 Hz, 1H), 7.85–7.84 (d, J=6.45 Hz, 1H), 2.65 (s, 6H), 0.87 (s, 6H). ^{13}C NMR (850 MHz, Chloroform-d): δ (ppm) 152.98, 141.70, 138.26, 132.29, 131.47, 131.15, 130.67, 129.59, 129.42, 128.93, 128.48, 127.45, 126.90, 126.30, 126.17, 125.74, 125.64, 124.89, 124.65, 123.84, 122.92, 122.89, 77.44, 77.23, 77.01, 12.74, 11.61. GC/HRMS (EI) calculated for $C_{29}H_{21}BCl_2F_2N_2$: 516.1142, found: 516.1140.

Synthesis of PY-BDP-2Br

N-Bromosuccinimide (NBS) (133 mg, 0.749mmol, 3 eq) in CH_2Cl_2 (10 mL) was slowly added dropwise to PY-BDP (112 mg, 0.249 mmol) in 25 mL of dry CH_2Cl_2 within 0.5 h. The resulting mixture was stirred for an additional 12 h, washed with a sodium chloride aqueous solution, and extracted with CH_2Cl_2. The organic layers were combined, dried with $MgSO_4$, and then evaporated until dryness. The purple solid product PY-BDP-2Br was obtained with a 46% yield (69.41 mg) through column chromatography on silica gel, using CH_2Cl_2/*n*-hexane (1:1, v/v) as the eluent. ^{1}H NMR (500 MHz, Chloroform-d): δ (ppm) 8.32–8.30 (d, J=7.85 Hz, 1H), 8.29–8.28 (d, J=7.60 Hz, 1H), 8.24–8.22 (d, J=7.45 Hz, 1H), 8.21–8.20 (d, J=8.95 Hz, 1H), 8.16–8.15 (d, J=8.95 Hz, 1H), 8.09–8.06 (m, 2H), 7.95–7.93 (d, J=9.10 Hz, 1H), 7.85–7.84 (d, J=7.75 Hz, 1H), 2.67 (s, 6H), 0.88 (s, 6H). ^{13}C NMR (850 MHz, Chloroform-d): δ (ppm) 154.40, 141.41, 140.90, 132.30, 131.48, 131.41, 131.16, 129.61, 129.41, 128.93, 128.63, 127.45, 126.90, 126.31, 126.18, 125.71, 125.67, 124.91, 124.66, 123.85, 112.08, 112.06, 77.48, 77.22, 76.97, 29.92, 29.90, 14.01, 13.36. GC/HRMS (EI) calculated for $C_{29}H_{21}BBr_2F_2N_2$: 604.0132, found: 606.0118.

Synthesis of PY-BDP-2I

N-Iodosuccinimide (NIS) (55 mg, 0.245 mmol, 5 eq) in CH_2Cl_2 (8 mL) was slowly added dropwise to PY-BDP (20 mg, 0.049 mmol) in 10 mL of dry CH_2Cl_2 within 0.5 h. The resulting mixture was stirred

for an additional 12 h, washed with a sodium chloride aqueous solution, and extracted with CH_2Cl_2. The organic layers were combined, dried with $MgSO_4$, and then evaporated until dryness. The red solid product PY-BDP-2I was obtained with a 68% yield (23.32 mg) through column chromatography on silica gel, using CH_2Cl_2/*n*-hexane (2:1, v/v) as the eluent. ^{1}H NMR (500 MHz, Chloroform-d): δ (ppm) 8.32–8.30 (d, J=7.90 Hz, 1H), 8.29–8.28 (d, J=7.75 Hz, 1H), 8.24–8.22 (d, J=7.45 Hz, 1H), 8.22–8.20 (d, J=8.95 Hz, 1H), 8.17–8.15 (d, J=8.95 Hz, 1H), 8.09–8.06 (m, 2H), 7.94–7.92 (d, J=9.10 Hz, 1H), 7.85–7.83 (d, J=7.75 Hz, 1H), 2.71 (s, 6H), 0.89 (s, 6H). ^{13}C NMR (850 MHz, Chloroform-d): δ (ppm) 156.99, 145.41, 140.48, 132.07, 131.26, 130.95, 129.39, 129.20, 128.79, 128.71, 127.24, 126.68, 126.07, 125.95, 125.49, 124.70, 124.44, 123.67, 85.75, 78.03, 77.93, 77.72, 77.15, 77.00, 76.86, 76.22, 76.00, 33.38, 31.93, 30.17, 30.04, 29.71, 29.37, 26.70, 22.70, 16.41, 16.14, 14.13. GC/HRMS (EI) calculated for $C_{29}H_{21}BF_2I_2N_2$: 699.9855, found: 699.9857.

Synthesis of BEN-BDP-2I

A solution of benzaldehyde (320 mg, 3.015 mmol, 1 eq) and 2,4-dimethylpyrrole (1.24 mL, 12.061 mmol, 4 eq) in dry CH_2Cl_2 (200 mL) was mixed with a solution of trifluoroacetic acid (46.17 μL, 0.603 mmol) in dry CH_2Cl_2 (3 mL) at room temperature under N_2 atmosphere. After 1.5 h, dichloro-5,6-dicyano-1,4-benzoquinone (DDQ) (0.68 g, 3.015 mmol) was added while cooling on ice and stirred for 10 min. After another hour, triethylamine (6 mL) was added followed by $BF_3{\cdot}Et_2O$ (6 mL), and the mixture was stirred for an additional 2 h before being poured into water. After extraction, the organic layer was dried over anhydrous $MgSO_4$, and then evaporated under reduced pressure to obtain the crude product. To purify the crude product, column chromatography was performed using silica gel and a mixture of CH_2Cl_2/*n*-hexane (1:1, v/v) as the eluent. This process produced an orange solid BEN-BDP, which was used as a precursor to BEN-BDP-2I.

N-Iodosuccinimide (NIS) (347 mg, 1.542 mmol, 5 eq) in CH_2Cl_2 (30 mL) was slowly added dropwise to BEN-BDP (100 mg, 0.308 mmol) in 25 mL of dry CH_2Cl_2 within 0.5 h. The resulting mixture was stirred for an additional 12 h, washed with a sodium chloride aqueous solution, and extracted with

CH_2Cl_2. The organic layers were combined, dried with $MgSO_4$, and then evaporated until dryness. The red solid product BEN-BDP-2I was obtained with a 71% yield (125 mg) through column chromatography on silica gel, using CH_2Cl_2/*n*-hexane (1:1, v/v) as the eluent. ^{1}H NMR (500 MHz, Chloroform-d): δ (ppm) 7.53–7.51 (m, 3H), 7.26–7.24 (m, 2H), 2.64 (s, 6H), 1.38 (s, 6H). ^{13}C NMR (850 MHz, Chloroform-d): δ (ppm) 156.96, 145.57, 141.58, 134.92, 131.49, 129.73, 129.66, 127.97, 85.87, 85.83, 77.47, 77.22, 76.96, 31.13, 29.90, 17.13, 16.22. GC/HRMS (EI) calculated for $C_{19}H_{17}BF_2I_2N_2$: 575.9542, found: 575.9541.

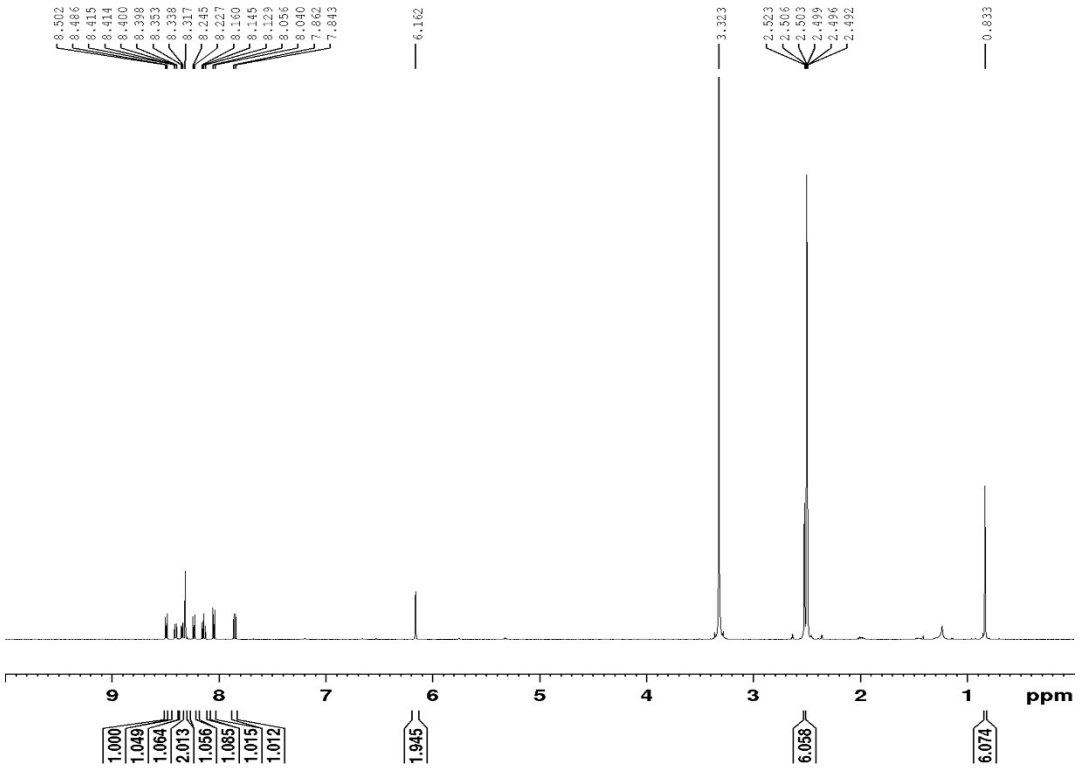

Fig. S1. ^{1}H NMR of PY-BDP.

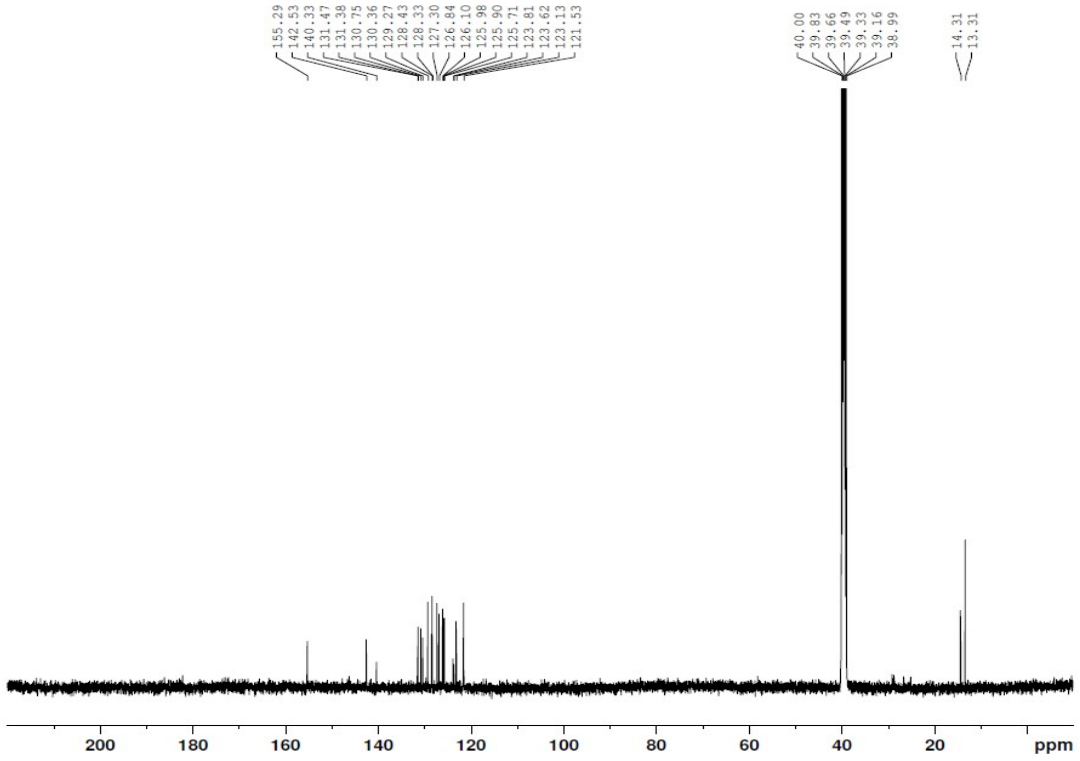

Fig. S2. ^{13}C NMR of PY-BDP.

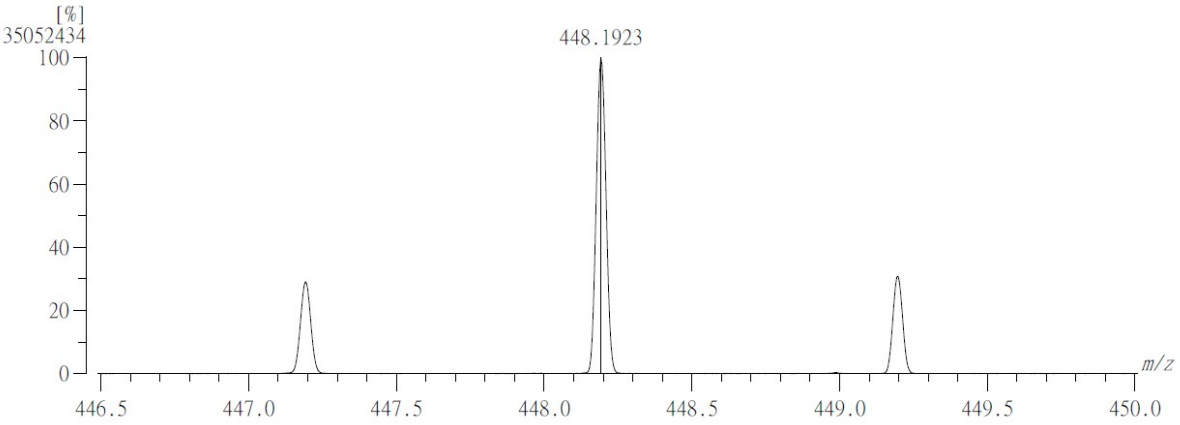

Fig. S3. GC/HRMS data of PY-BDP.

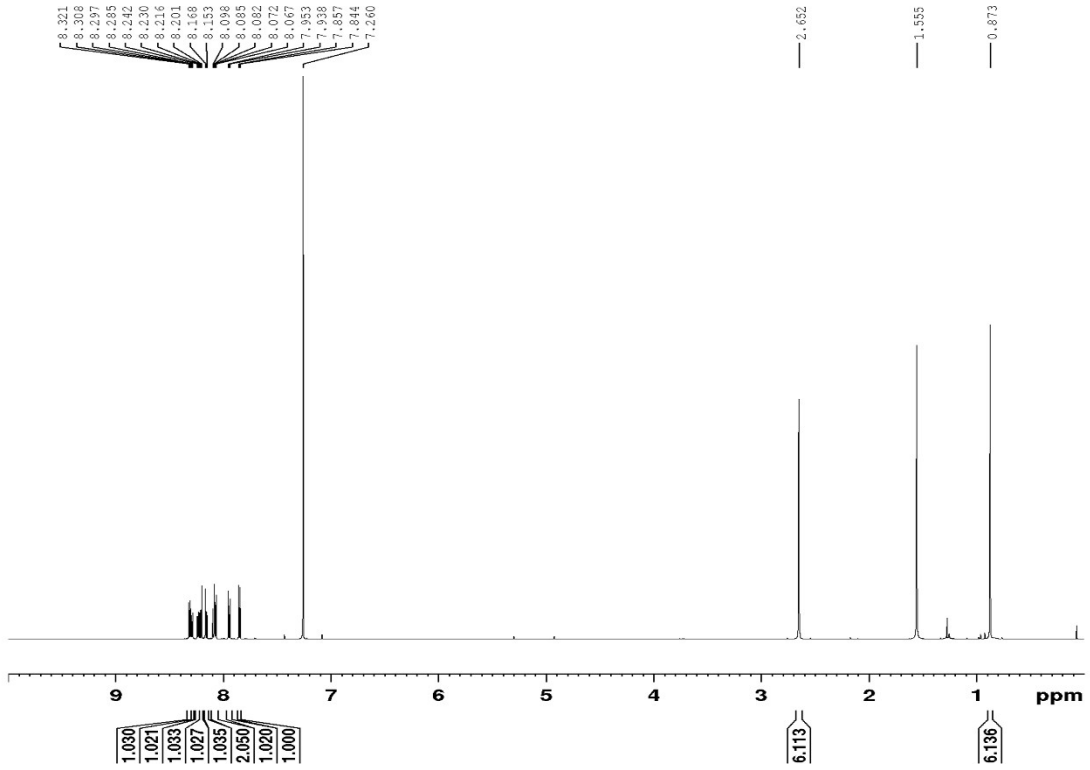

Fig. S4. [1]H NMR of PY-BDP-2Cl.

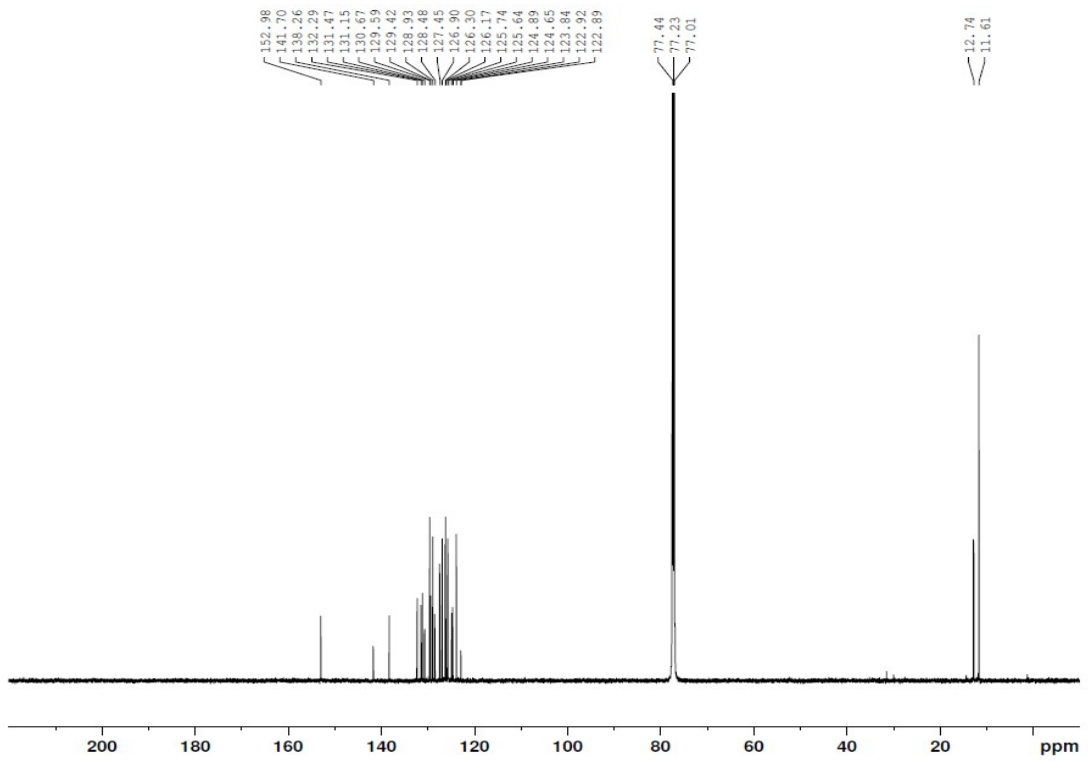

Fig. S5. [13]C NMR of PY-BDP-2Cl.

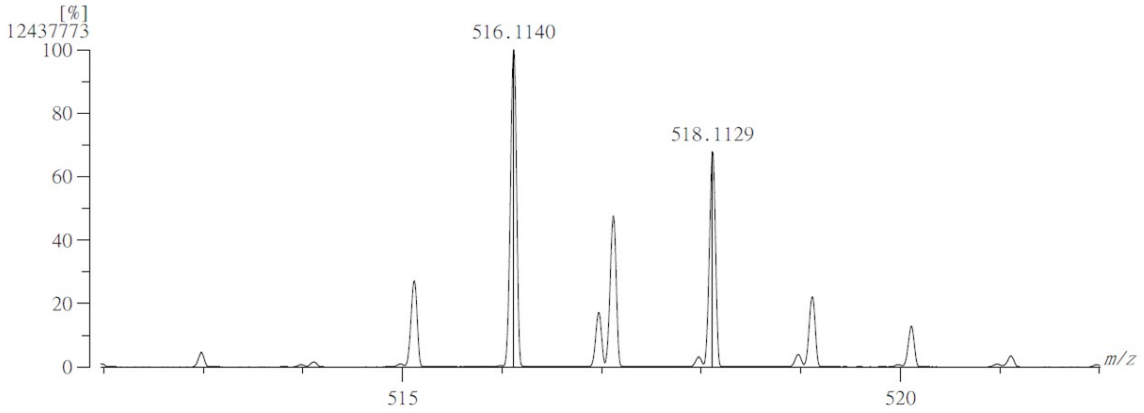

Fig. S6. GC/HRMS data of PY-BDP-2Cl.

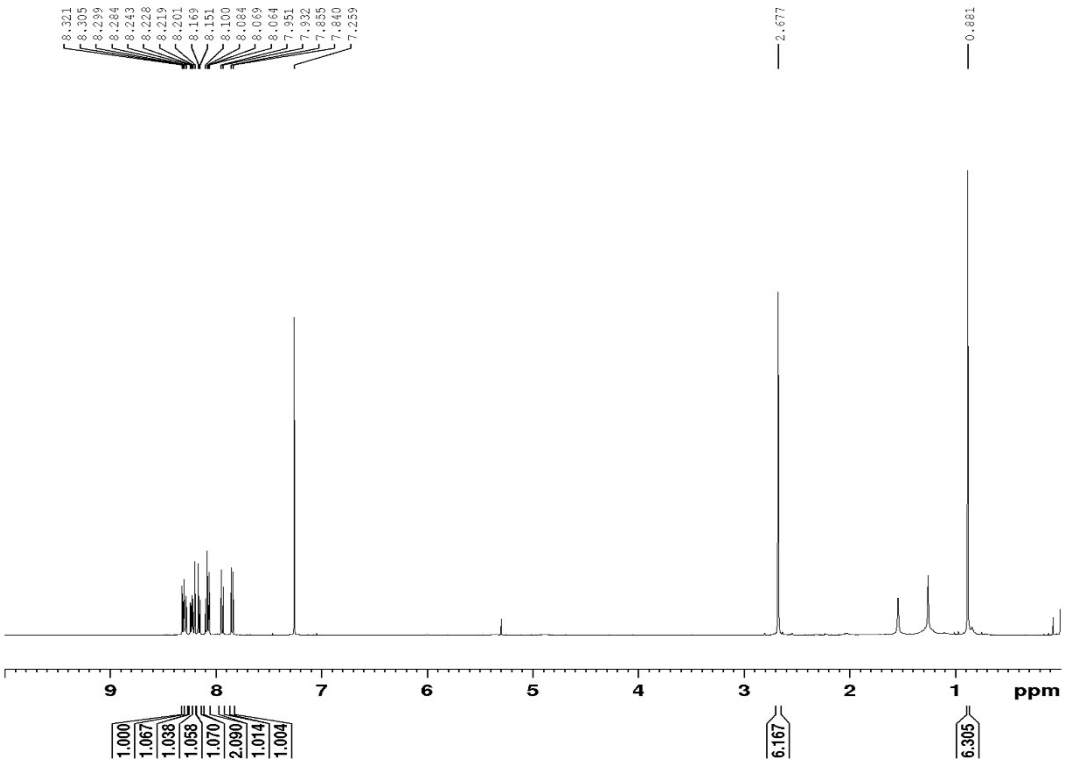

Fig. S7. ^{1}H NMR of PY-BDP-2Br.

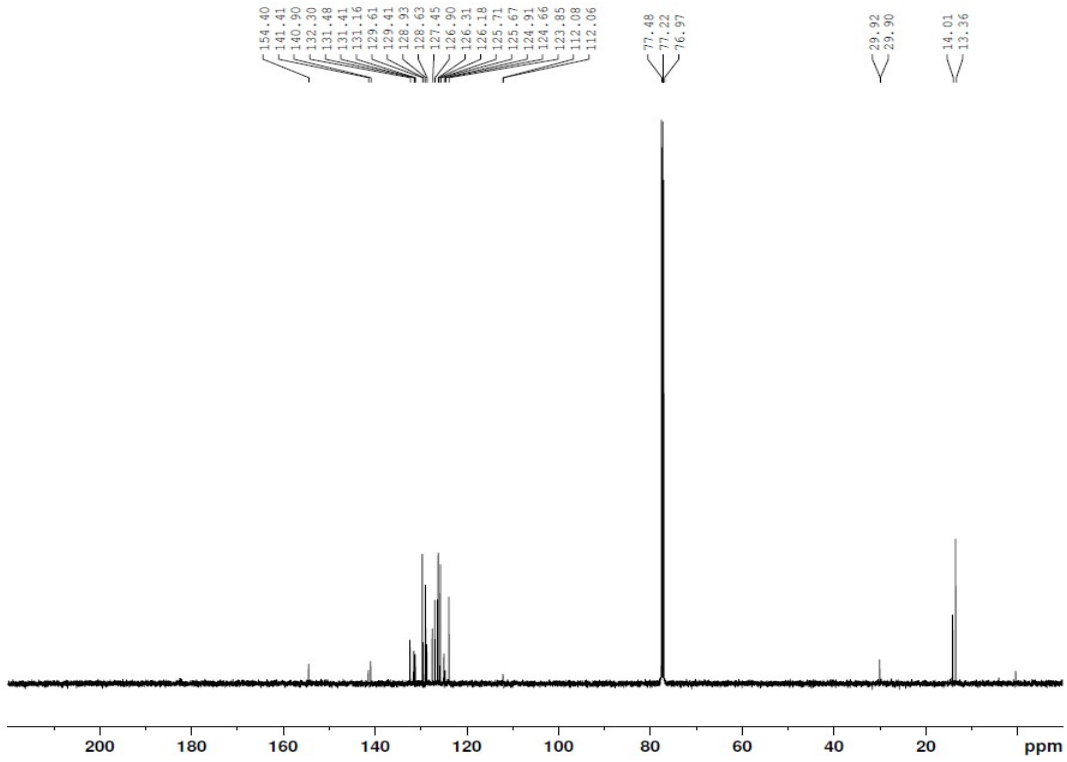

Fig. S8. ^{13}C NMR of PY-BDP-2Br.

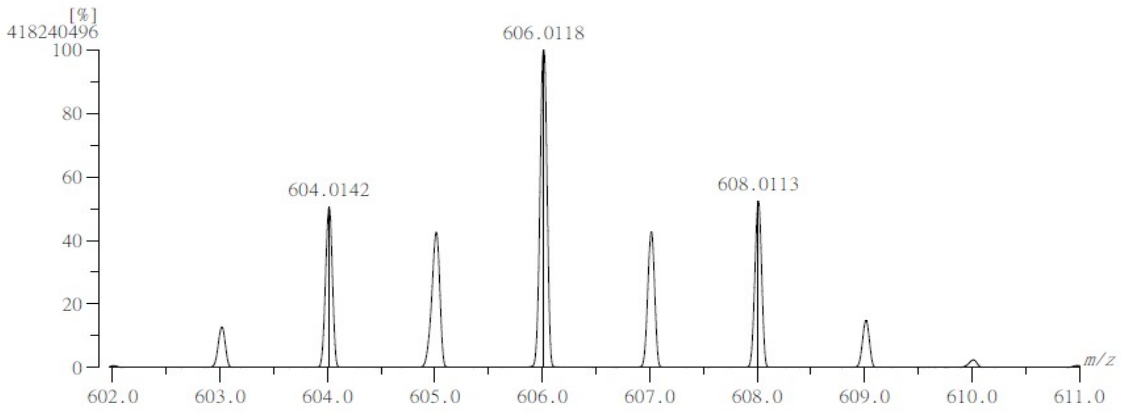

Fig. S9. GC/HRMS data of PY-BDP-2Br.

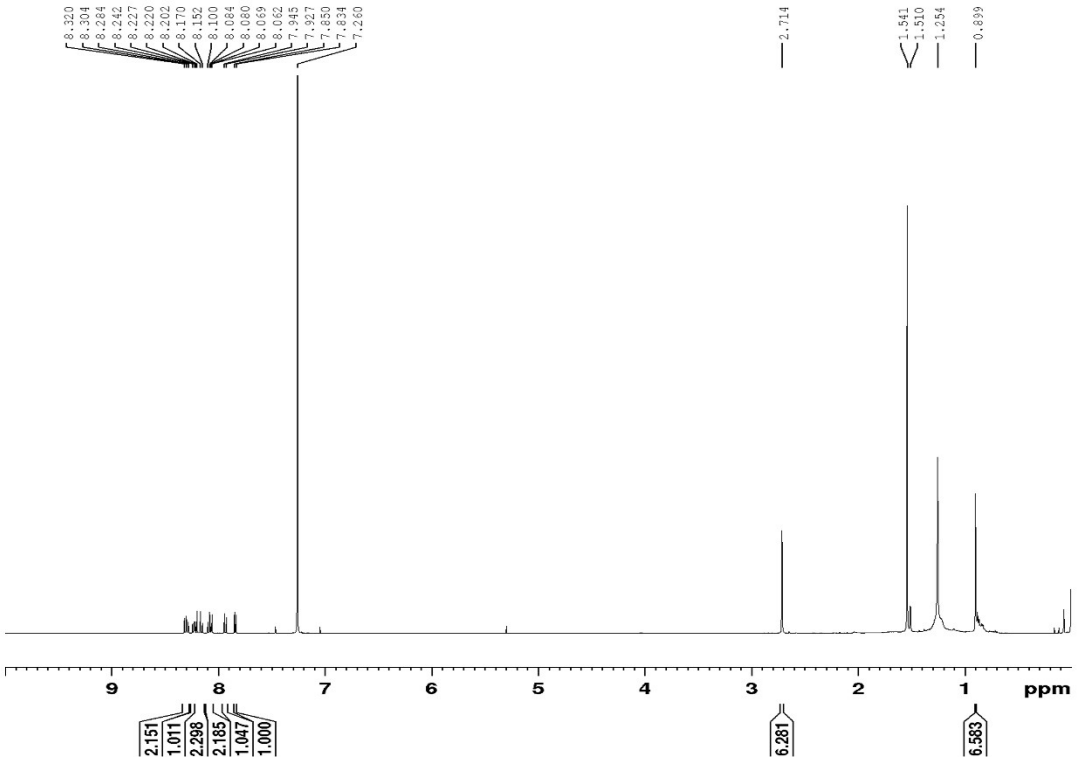

Fig. S10. [1]H NMR of PY-BDP-2I.

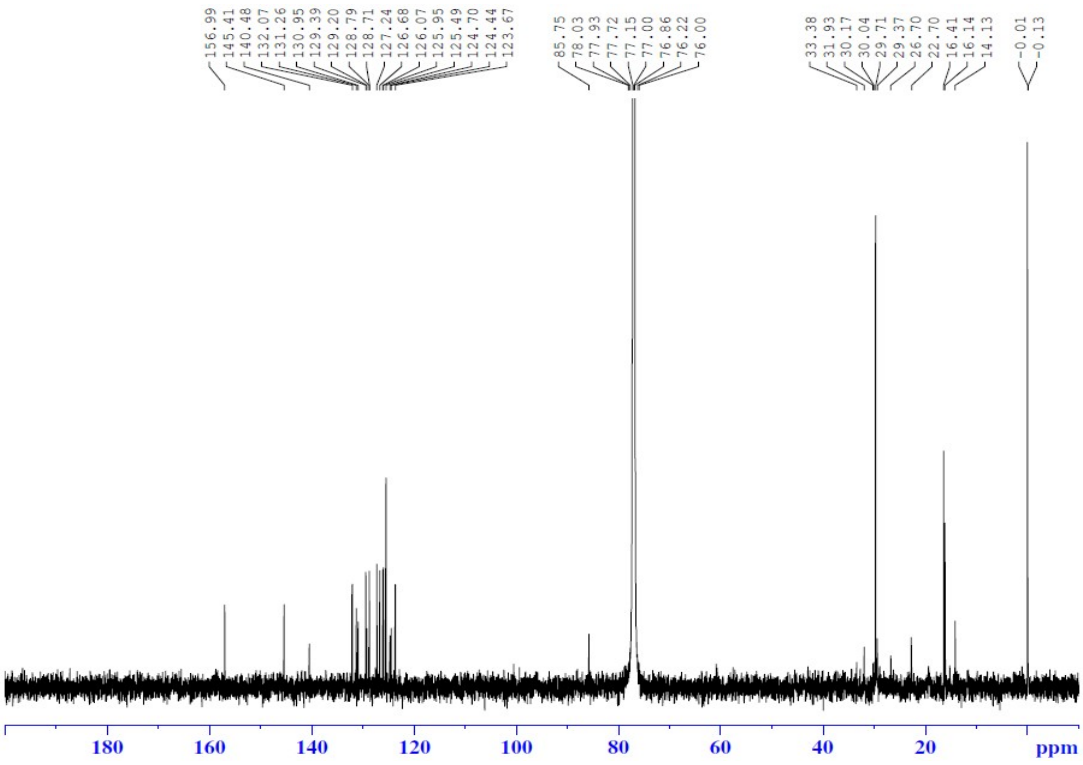

Fig. S11. [13]C NMR of PY-BDP-2I.

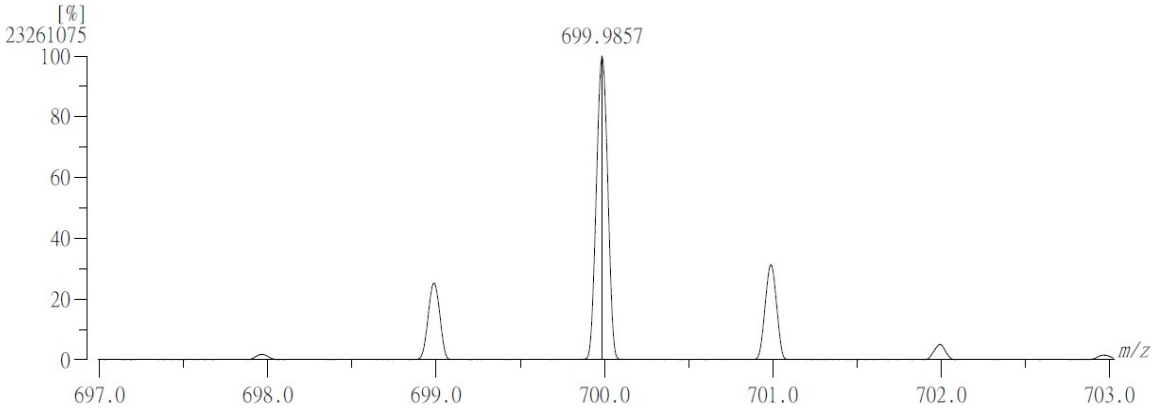

Fig. S12. GC/HRMS data of PY-BDP-2I.

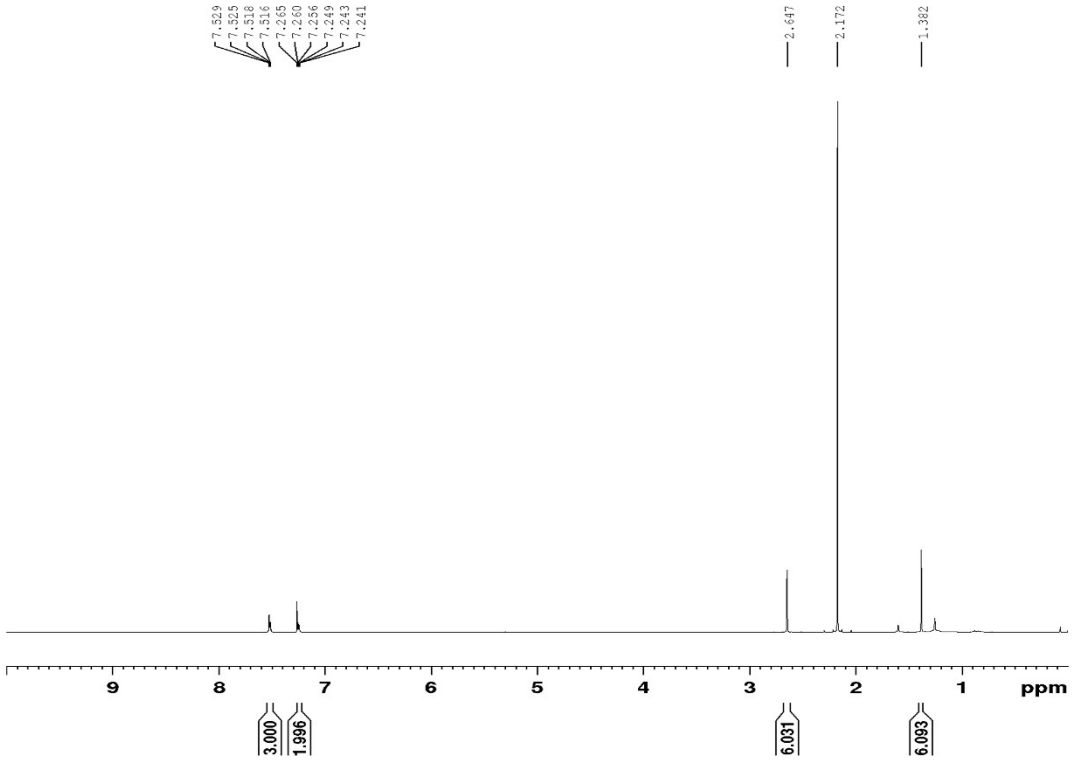

Fig. S13. ^{1}H NMR of BEN-BDP-2I.

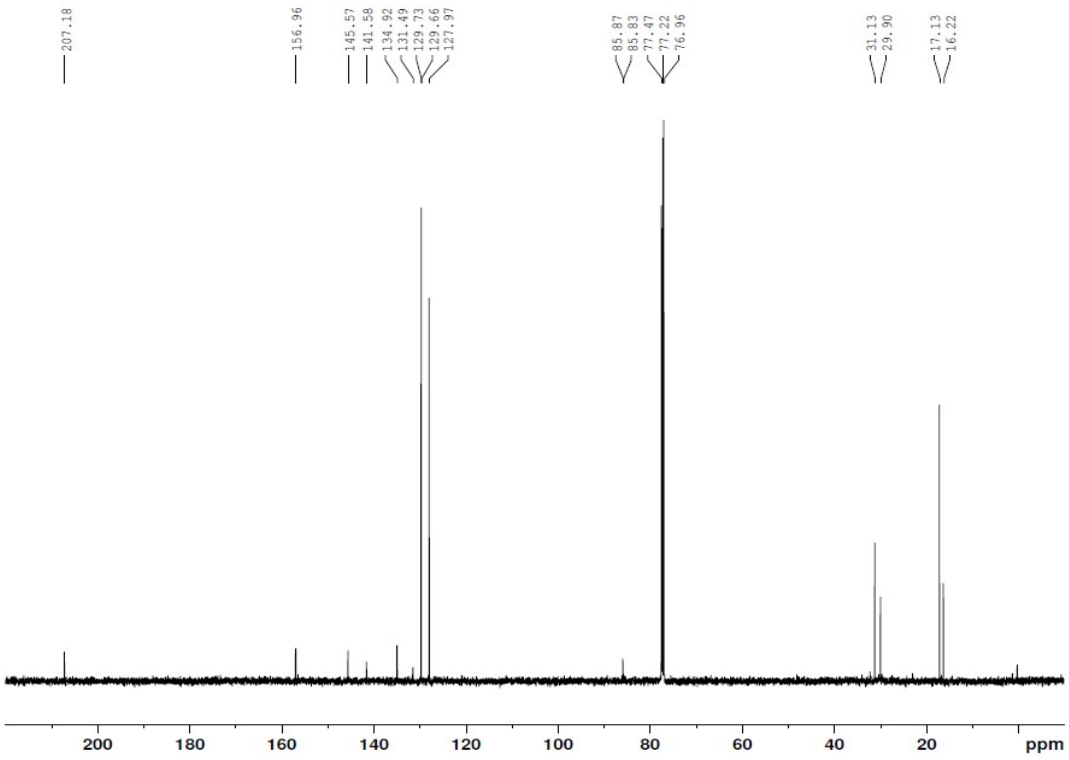

Fig. S14. ^{13}C NMR of BEN-BDP-2I.

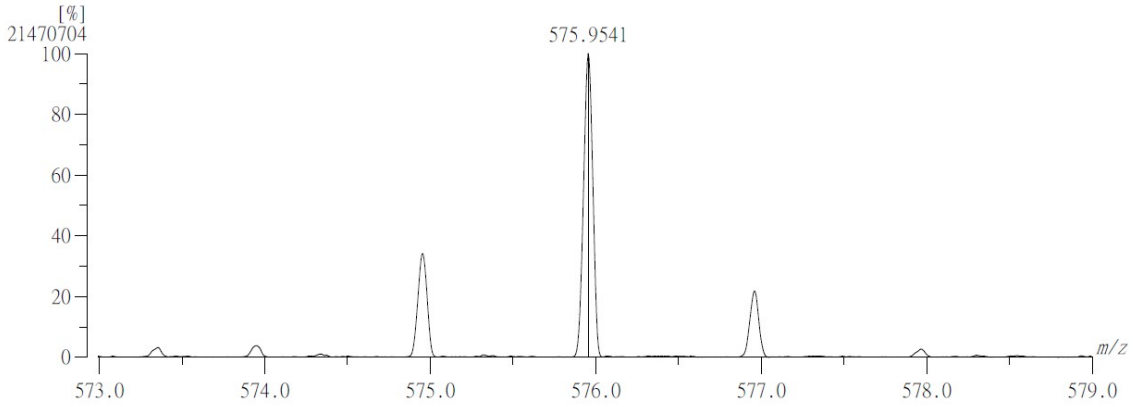

Fig. S15. GC/HRMS data of BEN-BDP-2I.

2. UV-vis absorption spectra

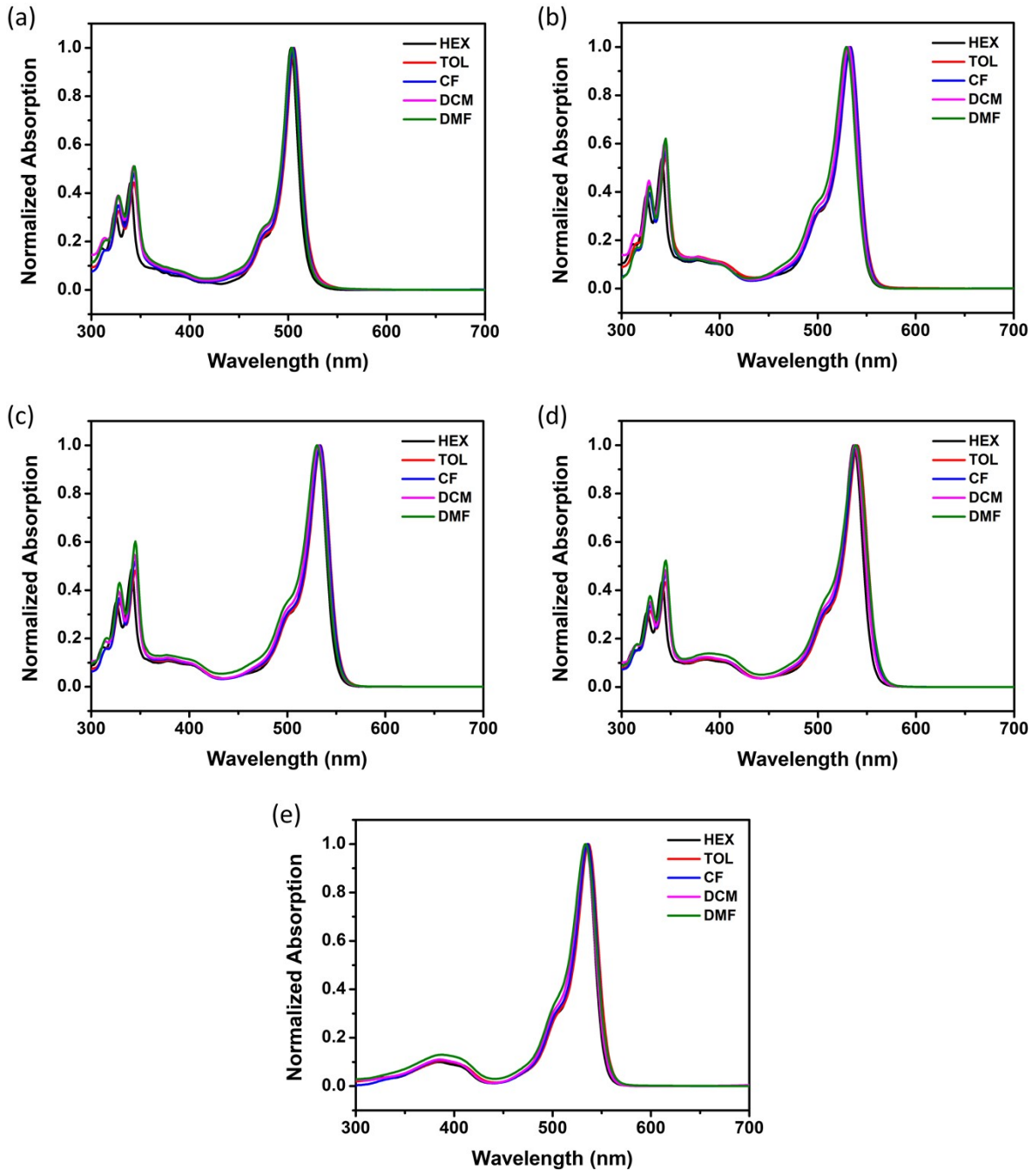

Fig. S16. Normalized UV-vis absorption spectra of (a) PY-BDP, (b) PY-BDP-2Cl, (c) PY-BDP-2Br, (d) PY-BDP-2I, and (e) BEN-BDP-2I in *n*-hexane (HEX), toluene (TOL), chloroform (CF), dichloromethane (DCM), and *N,N*-dimethylformamide (DMF).

3. Fluorescence emission spectra

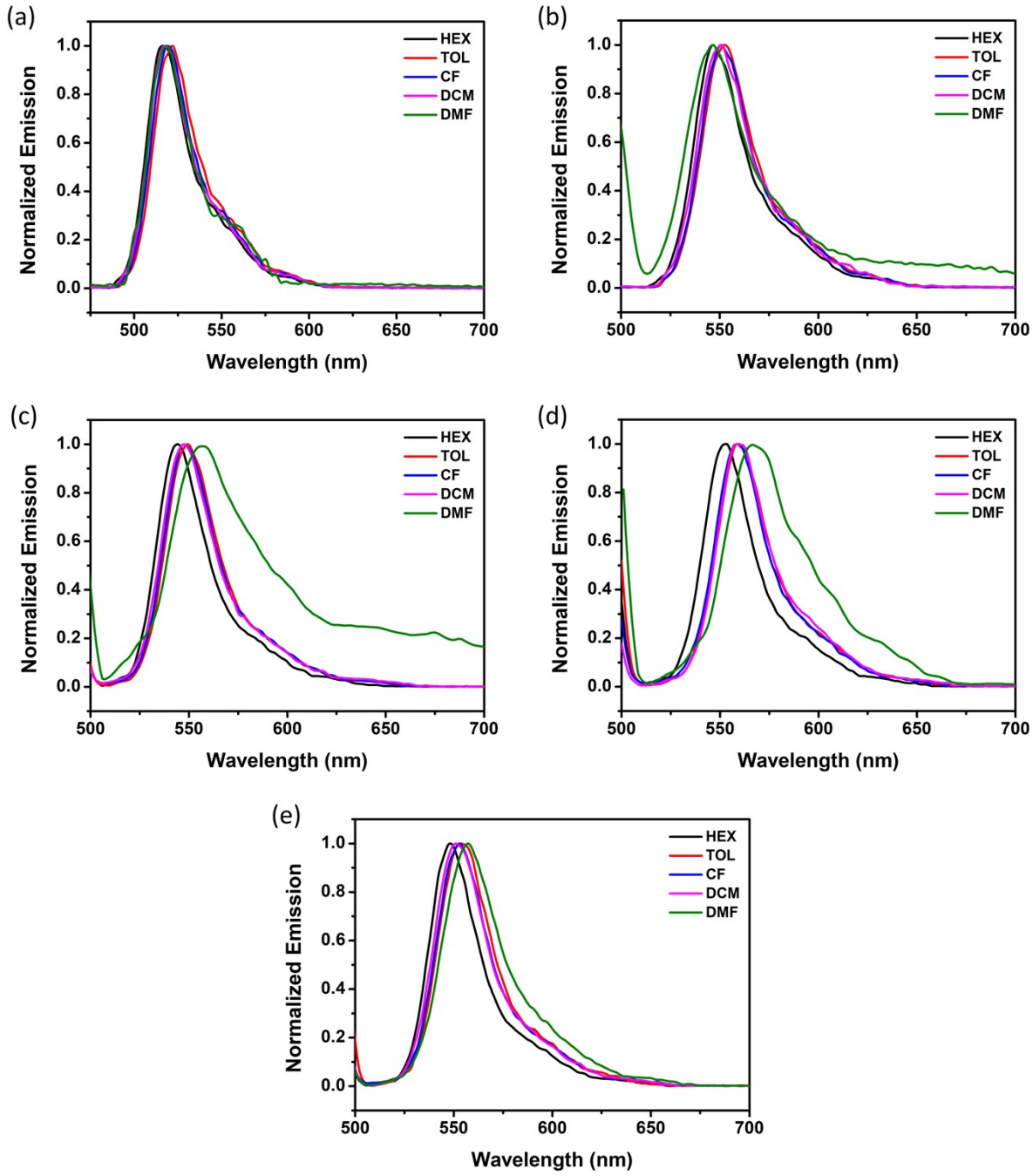

Fig. S17. Normalized fluorescence emission spectra of (a) PY-BDP, (b) PY-BDP-2Cl, (c) PY-BDP-2Br, (d) PY-BDP-2I, and (e) BEN-BDP-2I in different solvents.

Table S1. Absorption and fluorescence emission maximum wavelength, molar absorption coefficient, stokes shift, and fluorescence quantum yield of photosensitizers in different solvents

Compound	Solvent	λ_{abs} (nm)	ε_{max} (M^{-1} cm^{-1})	λ_{emi} (nm)	Δf (nm)	Φ_F
PY-BDP	HEX	503	40,100	516	13	0.890
	TOL	506	42,610	522	16	0.766
	CF	505	39,640	519	14	0.755
	DCM	504	38,970	517	13	0.630
	DMF	504	38,120	518	14	0.212
PY-BDP-2Cl	HEX	531	33,340	546	15	0.741
	TOL	533	32,980	552	19	0.723
	CF	533	31,700	550	17	0.710
	DCM	531	32,060	551	20	0.359
	DMF	529	28,230	546	17	0.100
PY-BDP-2Br	HEX	531	74,640	544	13	0.124
	TOL	534	72,970	549	15	0.109
	CF	533	70,760	547	14	0.106
	DCM	532	71,650	547	15	0.057
	DMF	530	62,260	559	29	0.014
PY-BDP-2I	HEX	537	92,160	553	16	0.023
	TOL	540	85,610	558	18	0.020
	CF	539	84,430	559	20	0.016
	DCM	538	87,870	559	21	0.014
	DMF	539	74,060	565	26	0.007
BEN-BDP-2I	HEX	534	111,920	548	14	0.049
	TOL	536	106,900	553	17	0.043
	CF	535	103,680	553	18	0.032
	DCM	534	105,520	551	17	0.027
	DMF	534	91,850	557	23	0.016

4. Singlet oxygen quantum yield (SOQY) measurement

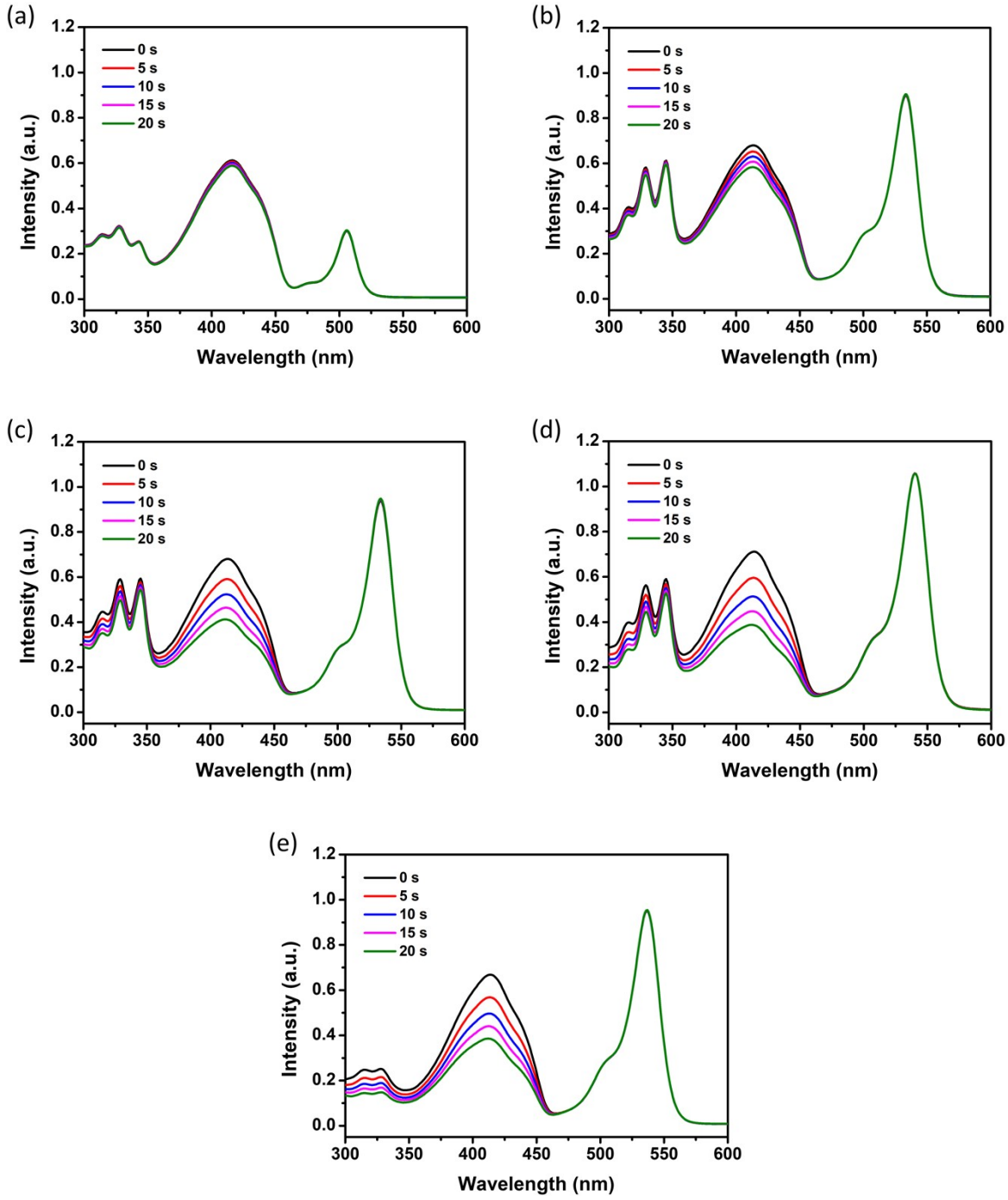

Fig. S18. The singlet oxygen quantum yield of (a) PY-BDP, (b) PY-BDP-2Cl, (c) PY-BDP-2Br, (d) PY-BDP-2I, and (e) BEN-BDP-2I was evaluated in toluene with an absorbance of 0.3 at 505 nm.

5. Electrochemical characterization

Table S2. Oxidation (E_{OX}) and reduction (E_{RED}) potentials of the reference compounds [a]

Compound	E_{OX} (V) [c]	E_{RED} (V) [c]
Pyrene	1.19	– [b]
BDP	– [b]	−0.99
BDP-2Cl	– [b]	−0.98
BDP-2Br	– [b]	−1.00
BDP-2I	– [b]	−1.01

[a] Cyclic voltammograms of the reference compounds in dichloromethane containing 0.10 M Bu_4NPF_6 as the supporting electrolyte and Ag/AgCl as the reference electrode. [b] Not observed. [c] Ferrocene (Fc) was used as the external reference ($E_{1/2}$ = +0.38 V, Fc^+ / Fc). Scan rates: 100 mV/s. c = 1.0 × 10^{-3} M, T = 25 °C.

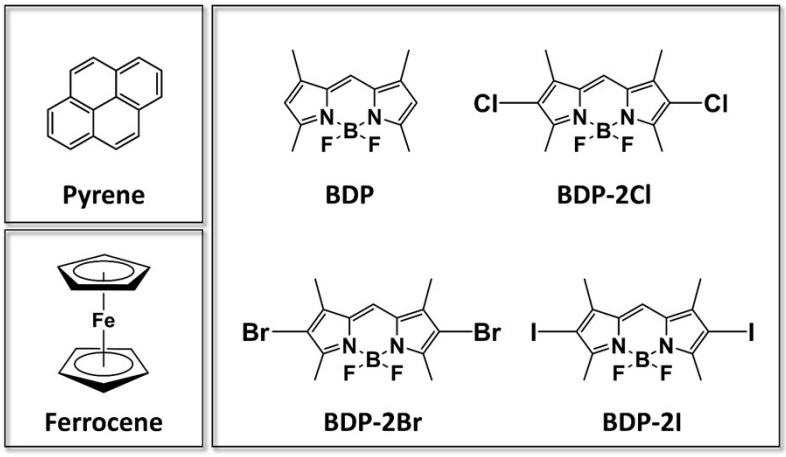

Fig. S19. Molecular design of the pyrene moiety (Pyrene) and the BODIPY moiety (BDP, BDP-2Cl, BDP-2Br, and BDP-2I).

6. fs-to-μs Transient absorption spectroscopy

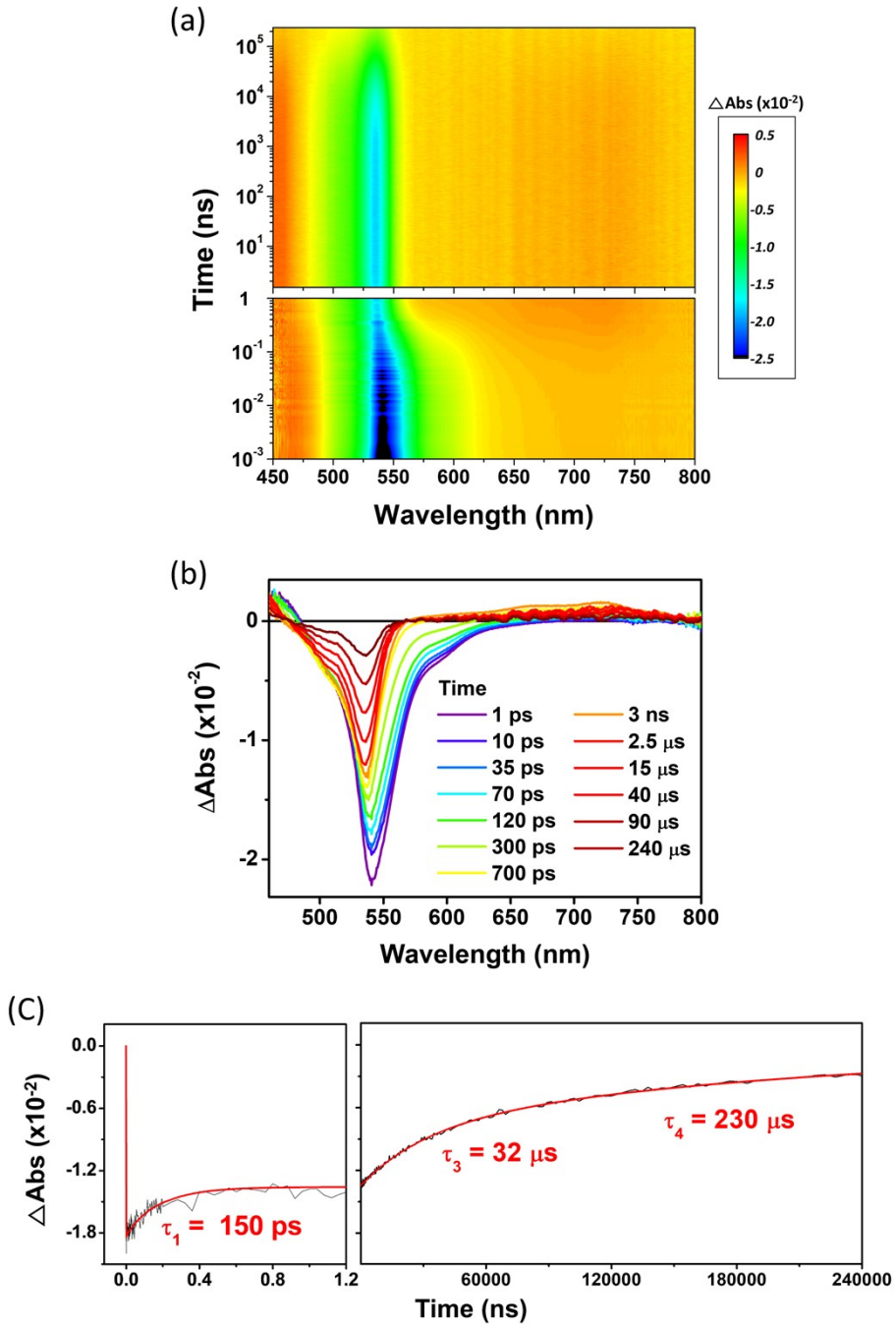

Fig. S20. fs-to-μs TA (a) 2D map, (b) spectra, and (c) decay profile of BEN-BDP-2I in toluene with photoexcitation at 500 nm. TA decay profile was plotted at 540 nm. Because our measured time window, 240 μs, is not enough to measure the longest decay time constant, we estimated the other time constants with the last infinite time constant.

7. Density functional theory (DFT) calculation

1) Optimized geometry of PY-BDP

1	C	−1.73043	1.22246	−0.28565
2	N	−3.07772	1.24424	0.09943
3	B	−3.97232	0.00089	0.35697
4	N	−3.07859	−1.24345	0.10118
5	C	−1.73129	−1.22311	−0.28393
6	C	−1.06562	−0.00067	−0.47718
7	C	−1.28901	2.58237	−0.41124
8	C	−2.38966	3.37283	−0.09782
9	C	−3.47427	2.52851	0.21169
10	C	−3.47592	−2.52731	0.21550
11	C	−2.39181	−3.37278	−0.09261
12	C	−1.29067	−2.58348	−0.40726
13	C	0.36298	−0.00144	−0.92249
14	C	1.42492	−0.00028	0.01055
15	C	2.77220	−0.00085	−0.47162
16	C	3.03404	−0.00255	−1.87601
17	C	1.94969	−0.00367	−2.76710
18	C	0.64100	−0.00313	−2.29476
19	C	0.06113	3.11537	−0.78777
20	C	0.05920	−3.11789	−0.78281
21	C	−4.86377	−2.91063	0.61100
22	C	−4.86175	2.91325	0.60711
23	F	−5.06121	0.00065	−0.51996
24	F	−4.42762	0.00204	1.67913
25	C	1.20775	0.00146	1.43396
26	C	2.25018	0.00253	2.31029
27	C	3.61313	0.00200	1.85689
28	C	3.86266	0.00030	0.45096
29	C	5.20856	−0.00025	−0.02936
30	C	5.43565	−0.00196	−1.44877
31	C	4.39799	−0.00305	−2.32981
32	C	4.70060	0.00310	2.74565
33	C	6.01006	0.00255	2.26803
34	C	6.26401	0.00090	0.89733
35	H	−2.42024	4.45417	−0.08868
36	H	−2.42300	−4.45408	−0.08160
37	H	2.13911	−0.00495	−3.83671
38	H	−0.18561	−0.00398	−2.99881
39	H	0.03596	4.20813	−0.79695
40	H	0.83580	2.80160	−0.08124
41	H	0.37847	2.77405	−1.77748
42	H	0.37565	−2.78046	−1.77415
43	H	0.83448	−2.80131	−0.07822
44	H	0.03404	−4.21068	−0.78770
45	H	−4.96613	−3.99674	0.64212
46	H	−5.11095	−2.49716	1.59357
47	H	−5.59156	−2.50027	−0.09571
48	H	−5.59023	2.49816	−0.09606
49	H	−5.10722	2.50523	1.59243

50	H	−4.96479	3.99944	0.63232
51	H	0.18839	0.00190	1.80463
52	H	2.06216	0.00383	3.38044
53	H	6.46136	−0.00237	−1.80719
54	H	4.58413	−0.00434	−3.40022
55	H	4.50963	0.00439	3.81515
56	H	6.83911	0.00342	2.96922
57	H	7.28743	0.00049	0.53255

2) Optimized geometry of PY-BDP-2Cl

1	C	1.27930	−1.22173	−0.15088
2	N	2.67714	−1.24529	−0.09052
3	B	3.60400	0.00032	−0.04734
4	N	2.67665	1.24567	−0.08913
5	C	1.27885	1.22152	−0.15078
6	C	0.58889	−0.00023	−0.18341
7	C	0.81019	−2.57483	−0.17190
8	C	1.96189	−3.35119	−0.12441
9	C	3.10148	−2.52133	−0.07501
10	C	3.10046	2.52188	−0.07453
11	C	1.96058	3.35126	−0.12577
12	C	0.80924	2.57443	−0.17333
13	C	−0.90416	−0.00054	−0.27045
14	C	−1.70327	0.00075	0.93745
15	C	−3.12605	0.00059	0.81006
16	C	−3.73686	−0.00084	−0.47752
17	C	−2.92571	−0.00219	−1.64850
18	C	−1.50029	−0.00202	−1.49519
19	C	−5.15802	−0.00097	−0.60015
20	C	−5.72922	−0.00242	−1.88125
21	C	−4.92803	−0.00374	−3.01940
22	C	−3.54079	−0.00362	−2.90924
23	C	−3.94381	0.00186	1.98027
24	C	−5.37229	0.00172	1.82530
25	C	−5.95178	0.00038	0.59670
26	C	−1.13804	0.00203	2.22210
27	C	−1.94577	0.00324	3.35594
28	C	−3.33125	0.00319	3.24147
29	C	−0.58856	−3.10072	−0.22892
30	C	−0.58968	3.09971	−0.23174
31	C	4.53565	2.91272	−0.01999
32	C	4.53682	−2.91118	−0.01769
33	F	4.35686	−0.00092	1.13544
34	H	−0.88793	−0.00302	−2.39080
35	H	−6.80951	−0.00253	−1.97760
36	H	−5.38872	−0.00486	−4.00056
37	H	−2.92329	−0.00465	−3.80077
38	H	−5.98504	0.00270	2.72034

39	H	−7.03207	0.00028	0.49918
40	H	−0.06084	0.00207	2.33390
41	H	−1.48665	0.00423	4.33778
42	H	−3.95147	0.00416	4.13115
43	H	−0.57933	−4.18708	−0.14087
44	H	−1.20481	−2.69849	0.57714
45	H	−1.07744	−2.84069	−1.17061
46	H	−1.07879	2.83629	−1.17235
47	H	−1.20553	2.70002	0.57591
48	H	−0.58077	4.18636	−0.14734
49	H	4.63445	3.99421	0.05441
50	H	5.02403	2.44394	0.83685
51	H	5.05761	2.56670	−0.91582
52	H	5.07030	−2.52373	−0.88906
53	H	5.01180	−2.48006	0.86646
54	H	4.63762	−3.99462	0.01145
55	F	4.46328	0.00171	−1.15387
56	Cl	2.02380	5.09180	−0.12856
57	Cl	2.02561	−5.09173	−0.12521

3) Optimized geometry of PY-BDP-2Br

1	C	1.03678	−1.22180	−0.13141
2	N	2.43424	−1.24508	−0.06672
3	B	3.36061	0.00100	−0.02096
4	N	2.43333	1.24648	−0.06517
5	C	1.03591	1.22218	−0.13090
6	C	0.34606	−0.00005	−0.16597
7	C	0.56823	−2.57563	−0.15428
8	C	1.72035	−3.35358	−0.10362
9	C	2.85928	−2.52110	−0.05046
10	C	2.85742	2.52283	−0.04924
11	C	1.71792	3.35446	−0.10360
12	C	0.56640	2.57568	−0.15455
13	C	−1.14666	−0.00059	−0.25848
14	C	−1.95034	−0.00001	0.94643
15	C	−3.37261	−0.00047	0.81373
16	C	−3.97860	−0.00149	−0.47613
17	C	−3.16305	−0.00209	−1.64404
18	C	−1.73823	−0.00164	−1.48538
19	C	−5.39929	−0.00193	−0.60408
20	C	−5.96569	−0.00295	−1.88733
21	C	−5.16023	−0.00352	−3.02245
22	C	−3.77341	−0.00311	−2.90708
23	C	−4.19475	0.00008	1.98087
24	C	−5.62264	−0.00038	1.82055
25	C	−6.19752	−0.00133	0.58979
26	C	−1.38991	0.00089	2.23317
27	C	−2.20187	0.00141	3.36399

28	C	−3.58691	0.00103	3.24435
29	C	−0.83350	−3.09319	−0.21621
30	C	−0.83567	3.09219	−0.21737
31	C	4.29536	2.90426	0.00960
32	C	4.29750	−2.90115	0.01060
33	F	4.11015	−0.00005	1.16400
34	H	−1.12253	−0.00210	−2.37870
35	H	−7.04561	−0.00328	−1.98772
36	H	−5.61722	−0.00431	−4.00534
37	H	−3.15256	−0.00356	−3.79628
38	H	−6.23873	0.00004	2.71329
39	H	−7.27744	−0.00167	0.48821
40	H	−0.31314	0.00119	2.34897
41	H	−1.74641	0.00212	4.34753
42	H	−4.21045	0.00145	4.13171
43	H	−0.83140	−4.17927	−0.12583
44	H	−1.45084	−2.68517	0.58601
45	H	−1.31640	−2.83213	−1.16073
46	H	−1.31862	2.82867	−1.16116
47	H	−1.45255	2.68556	0.58593
48	H	−0.83427	4.17847	−0.12938
49	H	4.40216	3.98507	0.07972
50	H	4.77658	2.43518	0.87033
51	H	4.81813	2.54982	−0.88240
52	H	4.82896	−2.51377	−0.86206
53	H	4.76805	−2.46156	0.89287
54	H	4.40646	−3.98343	0.04515
55	F	4.22272	0.00249	−1.12536
56	Br	1.78840	5.25140	−0.10669
57	Br	1.79200	−5.25049	−0.10540

4) Optimized geometry of PY-BDP-2I

1	C	−1.22530	−0.84382	−0.14746
2	N	−1.24916	−2.24388	−0.08527
3	B	−0.00011	−3.16431	−0.06430
4	N	1.24901	−2.24399	−0.08531
5	C	1.22527	−0.84394	−0.14745
6	C	0.00001	−0.15252	−0.18385
7	C	−2.58178	−0.37150	−0.15601
8	C	−3.36543	−1.52303	−0.09697
9	C	−2.53086	−2.66441	−0.05554
10	C	2.53068	−2.66465	−0.05558
11	C	3.36534	−1.52335	−0.09693
12	C	2.58178	−0.37174	−0.15593
13	C	0.00008	1.34204	−0.27048
14	C	−0.00002	2.14258	0.93981
15	C	0.00005	3.56838	0.81317
16	C	0.00021	4.18168	−0.47658

17	C	0.00032	3.36935	−1.65055
18	C	0.00025	1.94137	−1.49845
19	C	0.00028	5.60601	−0.59914
20	C	0.00045	6.18006	−1.88312
21	C	0.00055	5.37725	−3.02548
22	C	0.00049	3.98561	−2.91480
23	C	−0.00006	4.38744	1.98649
24	C	0.00001	5.81880	1.83285
25	C	0.00017	6.40127	0.59995
26	C	−0.00017	1.57522	2.22721
27	C	−0.00027	2.38386	3.36561
28	C	−0.00021	3.77368	3.25124
29	C	−3.08412	1.03842	−0.21616
30	C	3.08424	1.03815	−0.21599
31	C	2.92898	−4.09970	0.03336
32	C	−2.92951	−4.09937	0.03330
33	F	−0.00011	−3.95266	1.09969
34	H	0.00032	1.32848	−2.39641
35	H	0.00050	7.26258	−1.97893
36	H	0.00069	5.83922	−4.00838
37	H	0.00057	3.36671	−3.80804
38	H	−0.00007	6.43262	2.72970
39	H	0.00022	7.48378	0.50341
40	H	−0.00021	0.49577	2.33864
41	H	−0.00038	1.92273	4.34883
42	H	−0.00029	4.39495	4.14283
43	H	−4.17212	1.05149	−0.12814
44	H	−2.67168	1.65147	0.58981
45	H	−2.81528	1.52204	−1.16034
46	H	2.81575	1.52173	−1.16030
47	H	2.67157	1.65128	0.58979
48	H	4.17221	1.05115	−0.12761
49	H	3.84860	−4.27257	−0.53115
50	H	3.12669	−4.37570	1.07675
51	H	2.14592	−4.75484	−0.34712
52	H	−2.14541	−4.75491	−0.34425
53	H	−3.13060	−4.37444	1.07628
54	H	−3.84741	−4.27259	−0.53393
55	F	−0.00019	−4.00221	−1.19731
56	I	5.47365	−1.61393	−0.05555
57	I	−5.47372	−1.61361	−0.05570

5) Optimized geometry of BEN-BDP-2I

1	C	1.22575	0.23789	0.02951
2	N	1.24847	−1.16368	0.02401
3	B	−0.00052	−2.08323	0.06171
4	N	−1.24946	−1.16275	0.04725
5	C	−1.22565	0.23862	0.02793

6	C	0.00018	0.93034	0.02967
7	C	2.58288	0.70818	0.02872
8	C	3.36514	−0.44598	0.01229
9	C	2.52954	−1.58689	0.01207
10	C	−2.53060	−1.58521	0.03415
11	C	−3.36538	−0.44395	0.00232
12	C	−2.58230	0.70964	−0.00470
13	C	0.00033	2.42572	0.02325
14	C	0.11004	3.12854	−1.18514
15	C	0.10718	4.52597	−1.18979
16	C	0.00093	5.23237	0.01259
17	C	−0.10574	4.53518	1.22033
18	C	−0.10927	3.13774	1.22634
19	C	3.09279	2.11708	0.04304
20	C	−3.08948	2.11916	−0.03913
21	C	−2.92783	−3.02335	0.02572
22	I	5.47341	−0.53775	−0.03319
23	C	2.92567	−3.02498	−0.02096
24	F	−0.01184	−2.93027	−1.06016
25	F	0.01041	−2.86219	1.23615
26	H	0.19417	2.58091	−2.11964
27	H	0.18951	5.06074	−2.13158
28	H	0.00124	6.31842	0.00846
29	H	−0.18775	5.07714	2.15803
30	H	−0.19356	2.59724	2.16496
31	H	4.16883	2.12186	0.22810
32	H	2.91581	2.61918	−0.91399
33	H	2.60890	2.71870	0.81558
34	H	−2.61781	2.70327	−0.83293
35	H	−4.16836	2.12332	−0.20608
36	H	−2.89345	2.64087	0.90322
37	H	−3.85233	−3.16347	0.59130
38	H	−3.11599	−3.36030	−1.00137
39	H	−2.14791	−3.65434	0.45095
40	H	2.14862	−3.66183	0.40090
41	H	3.10478	−3.34677	−1.05454
42	H	3.85449	−3.17428	0.53493
43	I	−5.47362	−0.53742	−0.04449

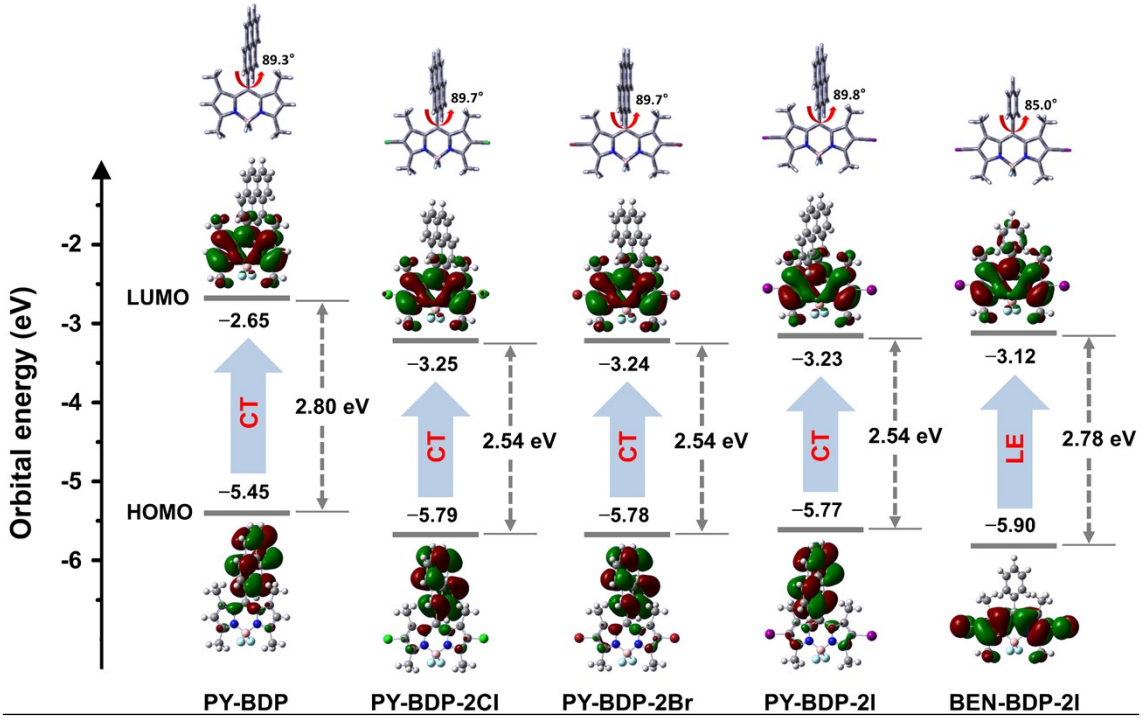

Fig. S21. The optimized geometry and frontier molecular orbitals of photosensitizers with transition types of charge transfer (CT) or locally excited (LE)

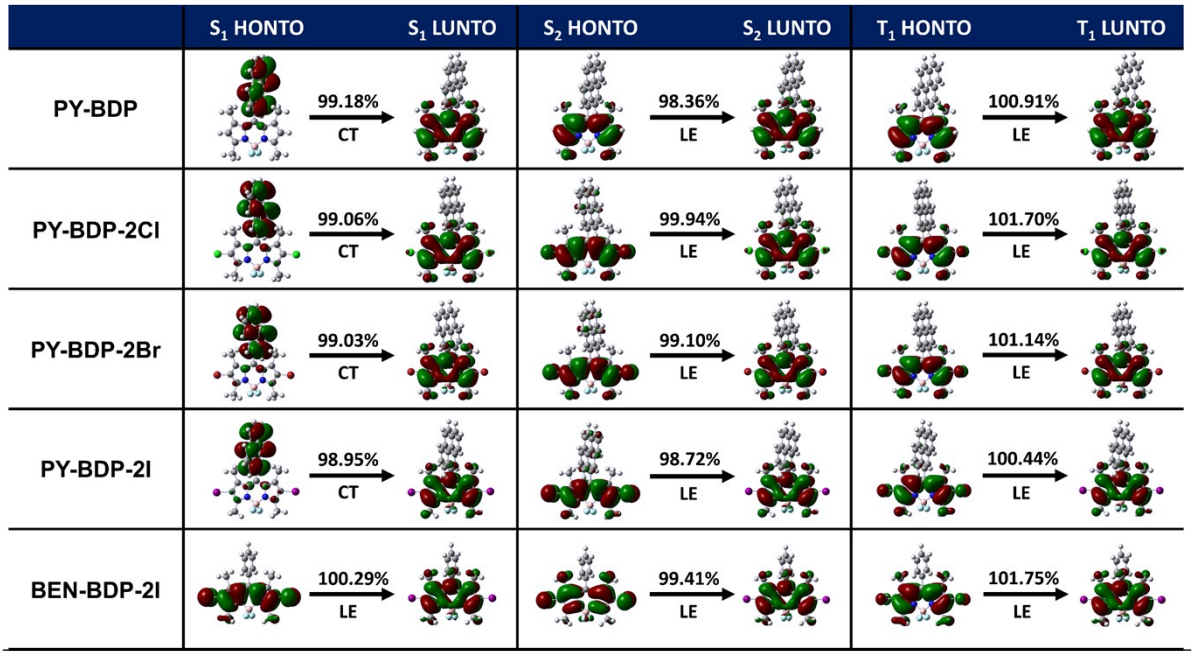

Fig. S22. Highest occupied natural transition orbital (HONTO) and lowest unoccupied natural transition orbital (LUNTO) of compounds.

8. Spin–orbit coupling matrix element (SOCME) calculation

Table S3. Spin–orbit coupling matrix element (SOCME) calculated between singlet and triplet state of compounds

Compound	Singlet state	Triplet state	X-component (cm^{-1})	Y-component (cm^{-1})	Z-component (cm^{-1})	SOCME [a] (cm^{-1})
PY-BDP	S_0	T_1	0.06	0	0.24	0.25
	S_1	T_1	0	0.62	0	0.62
	S_1	T_2	0.33	0	−0.52	0.61
PY-BDP-2Cl	S_0	T_1	0.04	0.01	0.14	0.14
	S_1	T_1	0	−0.88	0	0.88
	S_1	T_2	−0.18	0	0.13	0.22
PY-BDP-2Br	S_0	T_1	0.04	0.08	1.31	1.31
	S_1	T_1	0	−3.56	0	3.56
	S_1	T_2	0.32	0	0.17	0.36
PY-BDP-2I	S_0	T_1	0	−2.03	4.37	4.82
	S_1	T_1	8.48	0	0	8.48
	S_1	T_2	0	1.16	0.06	1.16

[a] It was calculated through the formula of $SOC = \sqrt{X^2 + Y^2 + Z^2}$ using the components of each axis value.

9. Triplet–triplet annihilation upconversion (TTA-UC)

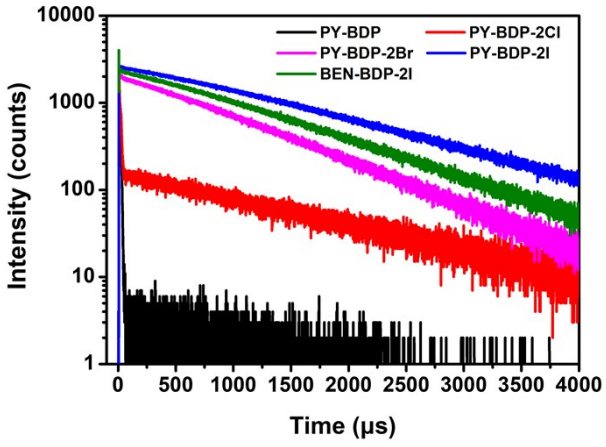

Fig. S23. The upconversion emission decay profiles of triplet photosensitizers (10 μM) and perylene (56 μM) in deoxygenated toluene were measured at 470 nm.

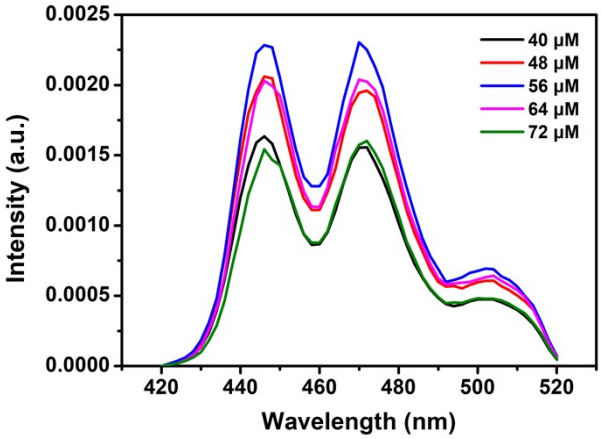

Fig. S24. UC emission spectra of PY-BDP-2I with various concentrations of perylene. The sensitizer concentration was fixed at 10 μM, while the concentrations of perylene were selected as 40, 48, 56, 64, and 72 μM.